Appendix A

Unitarity of the depth extrapolation operator

In prestack migration the location of the reflector's image is inferred from the wavefield extrapolated into the subsurface from the surface. Therefore, the extrapolation operator plays a major role in prestack migration. Many extrapolation algorithms have been developed since the migration technique was introduced in exploration seismology. The desired properties of the extrapolation operator are accuracy up to high dip angle, accuracy with laterally varying velocity, and efficiency in implementation. Since we have been interested in the structural image through migration, the amplitude treatment of a migration algorithm has been overlooked. However, in order to obtain a lithological image that requires angle-dependent reflectivity images, the means of treating of amplitude treatment of a migration algorithm need to be examined.

The split-step Fourier method (Stoffa and Fokkema, 1990) is one of the one-way wavefield extrapolation methods. In this thesis, I used the split-step Fourier method for the extrapolation operator. The reason for choosing it as an extrapolation method is that it is accurate up to the high-dip angle and has pseudo-unitary property. This appendix is devoted to proving the pseudo-unitary property of the split-step Fourier method.

A.0.1 Depth extrapolation using split-step Fourier method

The split-step Fourier extrapolation (Stoffa and Fokkema, 1990) consists of two-step extrapolation, which is a phase shifting in the (k, ω) domain followed by an additional phase shifting in the (x, ω) domain.

Let us consider a simple case that consists of two depth levels of extrapolation. Then the forward operator can be expressed as follows:

$$W = F_t^* \exp^{-ip_1 \Delta z} F_x^* \exp^{-ip_2 \Delta z} F_x \exp^{-ip_1 \Delta z} F_x^* \exp^{-ip_2 \Delta z} F_x F_t, \tag{A.1}$$

where F_x and F_t represent the Fourier transform along the space and the time domains, respectively. The phases p_1 and p_2 quantify the amount of phase shift in the (x, ω) and in the (k, ω) domain, and are defined as follows:

$$p_1(x, \omega) = \omega \Delta u(x) \tag{A.2}$$

and

$$p_2(k, \omega) = \omega u_0 \sqrt{1 - \left(\frac{k}{\omega u_0}\right)^2} \tag{A.3}$$

where u_0 represents the reference slowness and $\Delta u(x)$ is a variation of the slowness from the reference slowness. Then the adjoint of the forward operator becomes

$$W^* = F_t^* F_x^* \exp^{ip_2 \Delta z} F_x \exp^{ip_1 \Delta z} F_x^* \exp^{ip_2 \Delta z} F_x \exp^{ip_1 \Delta z} F_t. \tag{A.4}$$

If we apply the adjoint operator after the forward operator as follows:

$$W^* W = F_t^* F_x^* P_2^* F_x P_1^* F_x^* P_2^* F_x P_1^* F_t F_t^* P_1 F_x^* P_2 F_x P_1 F_x^* P_2 F_x F_t \tag{A.5}$$

with $P_1 = \exp^{-ip_1 \Delta z}$ and $P_2 = \exp^{-ip_2 \Delta z}$, where P_1 is a unitary operator, but P_2 is a pseudo-unitary operator because we substitute 0 for the evanescent component when p_2 becomes imaginary. If I group the operators so that they are in the same domain, for example the (k, ω) domain, we get the following:

$$\begin{aligned} W^* W &= F_t^* F_x^* (P_2^*)(F_x P_1^* F_x^*)(P_2^*)(F_x P_1^* F_t F_t^* P_1 F_x^*)(P_2)(F_x P_1 F_x^*)(P_2) F_x F_t \\ &= F_t^* F_x^* I_p I I_p I I_p I I_p F_x F_t \\ &= F_t^* F_x^* I_p F_x F_t \end{aligned} \tag{A.6}$$

where I is the identity matrix and I_p is an idempotent matrix with some elements that are 1 and others that are zeros. Therefore, the split-step Fourier extrapolation is pseudo-unitary.

Appendix B

Datuming by wavefield depth extrapolation

Seismic data acquired in areas with irregular topography introduce a numerical problem for migration algorithms that are based on depth extrapolation. Since numerically efficient migration schemes are usually based on depth extrapolation algorithms that allow the extrapolation of a wavefield from a flat surface to another flat surface, datuming is required prior to migration. Datuming is a method of processing for extrapolation of a known wavefield at a specified datum of arbitrary shape to another specified datum, also of arbitrary shape. For small differences in elevation and slow velocity variations between the input datum and the output datum, static shifting is a sufficiently accurate datum correction procedure. However, for significant differences in elevations and a more complicated velocity model, the accuracy of the static solution may prove to be insufficient, and a more exact method should be used.

Berryhill (1979; 1984) presented a wave equation datuming scheme for poststack and prestack data using the Kirchhoff integral method. Following his work, various forms of the Kirchhoff integral solution to the wave equation have been used by different authors for migration (Wiggins, 1984; Shtivelman and Canning, 1988) and for layer replacement (Yilmaz and Lucas, 1986; Berryhill, 1986).

This appendix presents a datuming scheme that can be used with any depth extrapolation scheme such as the phase-shift (Gazdag, 1978), split-step (Stoffa and Fokkema, 1990), and finite-difference methods (Claerbout, 1985).

B.1 Wave equation datuming

In this appendix, the basic strategy for finding a datuming operator consists of first formulating a forward-modeling operator and then deriving the corresponding datuming operator by transposing and taking the complex conjugate of the forward-modeling operator. For poststack or zero offset sections, the forward modeling is an algorithm that extrapolates the wavefield upward from a flat surface to an irregular surface by the one-way wave equation, using half the velocity of the medium. The modeling algorithm is derived so that it can be used with any depth extrapolation technique, including the phase-shift, split-step Fourier, and finite-difference methods.

B.1.1 Forward modeling operator

In forward modeling, the wavefield recorded at each geophone along an irregular surface is the wavefield propagated up to the depth level where the geophones are located. It is necessary to stop the wavefield propagation after recording because the reflection coefficient at the surface is almost -1. To do so, I formulate the forward modeling operator by propagating the wavefield upward with a filter between extrapolation steps to stop the wavefield propagation where it is recorded. Then all wave fields from all depth levels where the geophones are located are summed together to produce the wavefield along the irregular surface. In order to explain the algorithm clearly and schematically, I use a simple topography model that has only eight geophone groups on an irregular surface, as illustrated in Figure B.1.

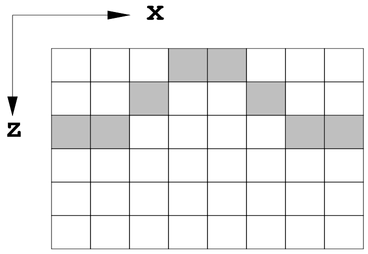

FIG. B.1. Synthetic surface recording geometry. Solid squares represent geophone location on an undulating surface. irrdtm-syngeometry [NR]

Figure B.2 schematically describes the forward modeling algorithm for the simple model. W_i represents upward extrapolation at the i-th depth level and F_1, F_2, and F_3

are spatial filters for grabbing the wavefield where the geophones are located at the corresponding depth levels. The operators $I - F_3$ and $I - F_2 - F_3$ in Figure B.2 stop propagating the wavefield at the locations where it is recorded below or at the corresponding depth level and keep propagating the wavefield at the locations where it is not yet recorded. Each small rectangle in Figure B.2 represents an abstract vector that contains wave fields at the corresponding space location. The wavefield along the irregular surface is obtained by summing the wave fields that are grabbed at the various depth levels.

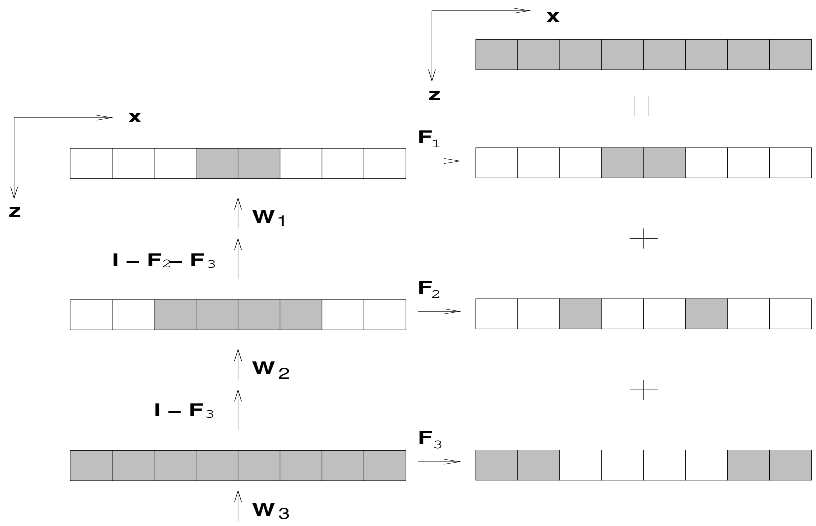

FIG. B.2. Forward modeling scheme: the schematic diagram for forward depth extrapolation when the surface is not flat. W_i represents the upward extrapolation operator at the i-th depth level. F_1, F_2, and F_3 are spatial filters shown in the text, and I is the identity matrix. irrdtm-tpfrdschm [NR]

The forward modeling scheme shown in Figure B.2 can be generalized algebraically, if we divide the topography into z levels, as follows:

$$\begin{bmatrix} d_0 \end{bmatrix} = \begin{bmatrix} I & 0 \end{bmatrix} G_1 E_1 G_2 E_2 \ldots G_{z-1} E_{z-1} G_z \begin{bmatrix} 0 \\ I \end{bmatrix} \begin{bmatrix} d_z \end{bmatrix} \tag{B.1}$$

$$E_i = \begin{bmatrix} I & 0 \\ 0 & W_i \end{bmatrix} \tag{B.2}$$

$$G_i = \begin{bmatrix} I & F_i \\ 0 & K_i \end{bmatrix} \tag{B.3}$$

where

$$K_i = I - \sum_{j=1}^{z-i} F_{z-j} \tag{B.4}$$

In equation (B.1), d_0 and d_z are wave fields on the irregular surface and the datum level, respectively. The extrapolation operator E is followed by the spatial filter G at every depth level. We can see that the upward extrapolation operator W_i is applied to the wavefield that does not arrive at the surface because the operator K_{i-1} removes the wavefield if it has arrived at any previous depth level. All wave fields that arrive at the surface are saved by the operator F_{i-1} for the final output. If a datum is located in the subsurface instead of at the surface, the operators K_i should not be used so that the wavefield keep propagating through. The operator K_i described in this appendix is a crude type of transmission coefficient. In order to implement the operator K_i more correctly, its diagonal elements should be the transmission coefficient according to the property of the interface and the incidence angle of wavefield instead of 1 or 0. However such a rigorous implementation of the transmission coefficient is not practical since it requires exhaustive ray tracing to find the incidence angle. It is generally accepted that the transmission coefficient is 1 on the interface between two solids and 0 on the interface between the solid and the air.

For the simple geometry shown in Figure B.1, F_1, F_2, and F_3 are simply diagonal matrices whose elements are 1 where the geophones are located and 0 elsewhere. Thus, their diagonal elements are as follows:

$$\begin{aligned} diag(F_1) &= \begin{bmatrix} 0 & 0 & 0 & 1 & 1 & 0 & 0 & 0 \end{bmatrix} \\ diag(F_2) &= \begin{bmatrix} 0 & 0 & 1 & 0 & 0 & 1 & 0 & 0 \end{bmatrix} \\ diag(F_3) &= \begin{bmatrix} 1 & 1 & 0 & 0 & 0 & 0 & 1 & 1 \end{bmatrix} \end{aligned}$$

The operator W_i in equation (B.2) can be any extrapolation scheme including the Kirchhoff, phase-shift, split-step, or finite-difference method. If we use the phase-shift extrapolation algorithm for W_i, we need an additional inverse Fourier transform in every extrapolation step because the operator G is in the space domain. However, all the other algorithms, such as the Kirchhoff, split-step, and finite-difference methods, do not need any additional computation, with the exception of the operation by G, which is the multiplication of the extrapolated wavefield by the zero/one filter.

B.1.2 Datuming operator

Now we can easily find the datuming operator by transposing and taking the complex conjugate of each matrix in the forward-modeling operator shown in equation (B.1). The datuming operator for a poststack data set gathered on an irregular surface is thus

$$\left[\begin{array}{c} d_z \end{array} \right] = \left[\begin{array}{cc} 0 & I \end{array} \right] G_z^T E_{z-1}^T G_{z-1}^T \ldots E_2^T G_2^T E_1^T G_1^T \left[\begin{array}{c} I \\ 0 \end{array} \right] \left[\begin{array}{c} d_0 \end{array} \right] \tag{B.5}$$

$$E_i^T = \left[\begin{array}{cc} I & 0 \\ 0 & W_i^T \end{array} \right] \tag{B.6}$$

$$G_i^T = \left[\begin{array}{cc} I & 0 \\ F_i & K_i \end{array} \right] \tag{B.7}$$

In equation (B.5), we can see that the downward extrapolation E^T is preceded by the filter G^T at every depth level. We then apply the downward extrapolation operator W_i^T to the wavefield that was introduced by the operator F_i up to a given depth level. The portion of the wavefield that is not introduced until a given depth level is removed by the operator K_i. Figure B.3 shows this datuming operator, while the topography is given by Figure B.1.

Coincidentally, this datuming scheme is the same as Reshef's (Reshef, 1991). He used the algorithm for depth migration from irregular surfaces with depth extrapolation. We can deduce that Reshef's algorithm assumes the same forward modeling algorithm as this one. By having both the forward operator and its adjoint we are prepared for inversion and velocity estimation.

B.1.3 Synthetic examples

I test the datuming scheme described above with phase-shift, split-step, and finite-difference depth extrapolation algorithms. For testing, I use a simple model, Figure B.4, that has a syncline reflector under an undulating surface. The irregular surface is modeled to have not only gradual topographic changes, but also discontinuity.

The forward modeling experiment was done using the algorithm explained in Figure B.2 for a constant velocity; Figure B.5(a) shows the result. Datuming was then performed using the algorithm shown in Figure B.3 with the phase-shift extrapolation as the depth

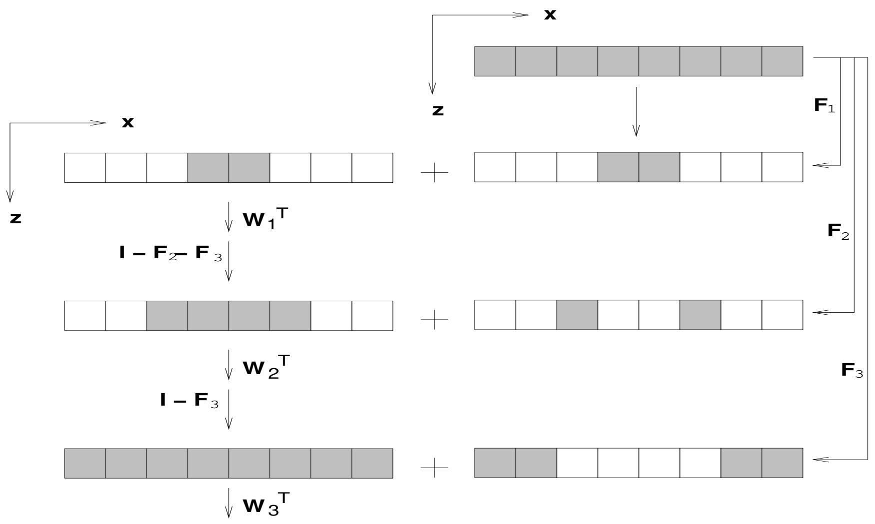

FIG. B.3. Datuming scheme: schematic diagram for the datuming operator as the conjugate to the forward extrapolation scheme, when the surfaces are irregular. W_1^T represents the downward propagation operator at each depth level. irrdtm-tpdtmschm [NR]

FIG. B.4. Synthetic model with a syncline reflector image (lower) under an undulating surface (upper). irrdtm-synmdl [R]

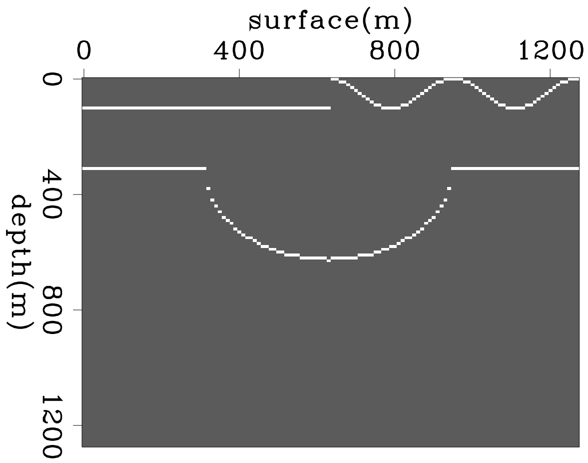

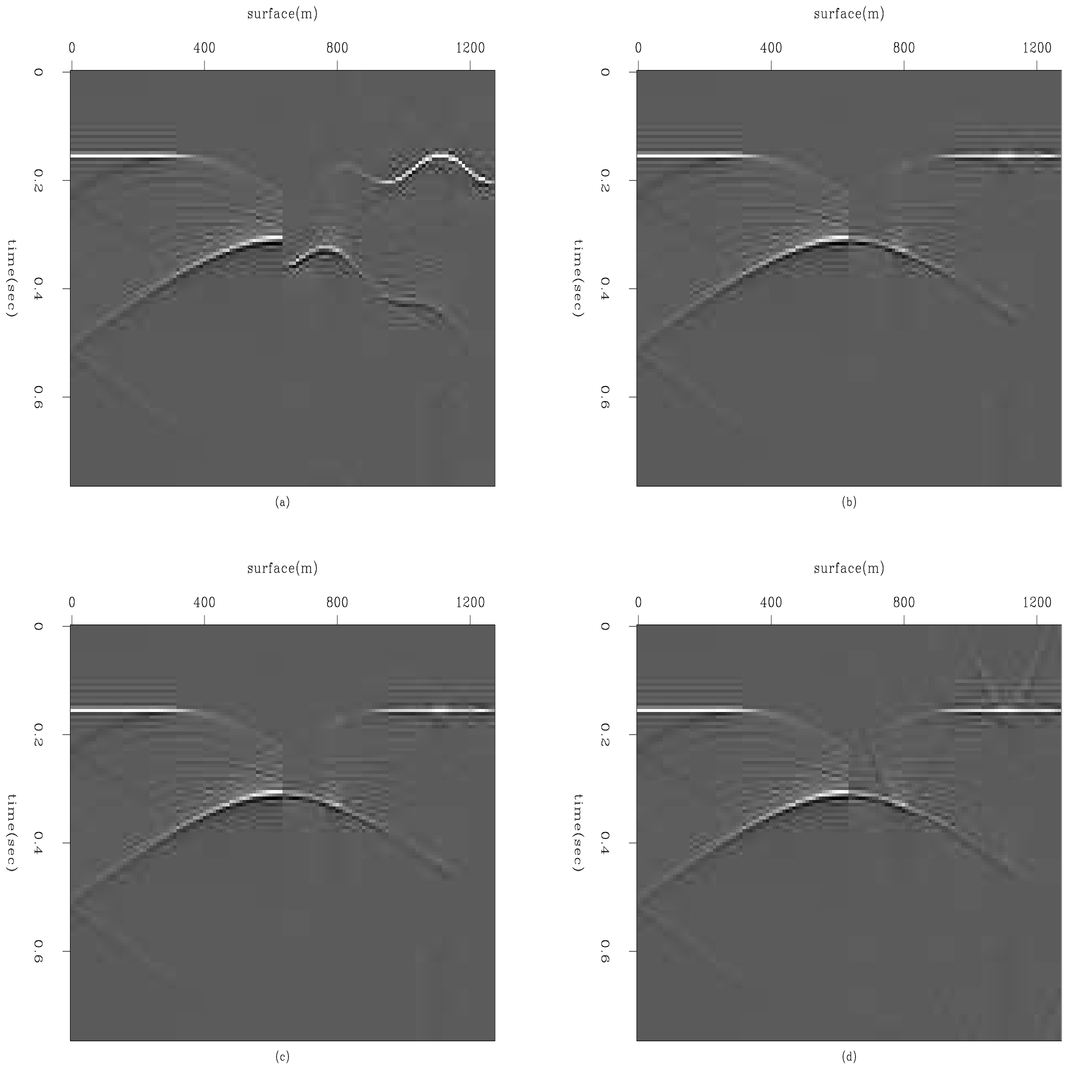

FIG. B.5. (a) Wave field recorded on the irregular surface using phase-shift extrapolation scheme. (b) Datumed wave field using phase-shift algorithm. (c) Datumed wave field using split-step algorithm. (d) Datumed wave field using 45-degree finite-difference algorithm. $\boxed{\text{irrdtm-datumgsw}}$ [R]

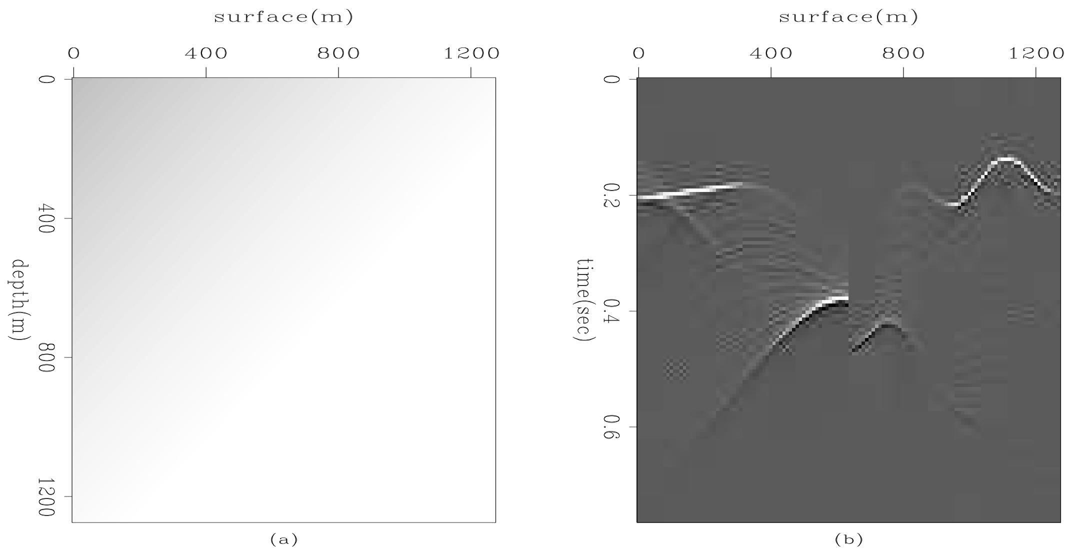

FIG. B.6. (a) velocity model, $v(x,z) = 1500. + 0.2x + 0.2z$. (b) Wave field recorded on the irregular surface using split-step extrapolation scheme. irrdtm-vxz-split-modl [R]

extrapolation operator W. The result appears in Figure B.5(b); the exact bow-tie shaped wave field is the characteristic of the syncline reflector on a flat datum. I then applied the same algorithm with the other depth extrapolation schemes. Figures B.5(c) and (d) show the datumed results for the split-step and the 45-degree finite-difference methods. When the velocity is constant, the split-step algorithm is identical to the phase-shift algorithm. Therefore, we can see that the datumed wave fields in Figures B.5(b) and (c) are the same. The result of the finite-difference method, Figure B.5(d), also shows a correctly-located bow-tie shaped wave field with remaining very weak artifacts in the region under the undulating surface. These artifacts can be explained as the energy from the evanescent region that has not been removed.

To illustrate the effectiveness of the datuming algorithm, I tested a velocity function that varies in depth and lateral extent for the same reflector and topographic model shown in Figure B.4. The velocity model used in this experiment has a linear increase both in depth and lateral: $v(x,z) = 1500. + 0.2x + 0.2z$ (Figure B.6(a)). The zero-offset data are modeled with the use of split-step extrapolation; Figure B.6(b) shows the result. The datuming algorithm is then applied to the data, Figure B.6(b), using the split-step extrapolation; the result is shown in Figure B.7(a). Figure B.7(b) shows the migrated image. By comparing Figure B.4 and Figure B.7(b), we can see the effect of the

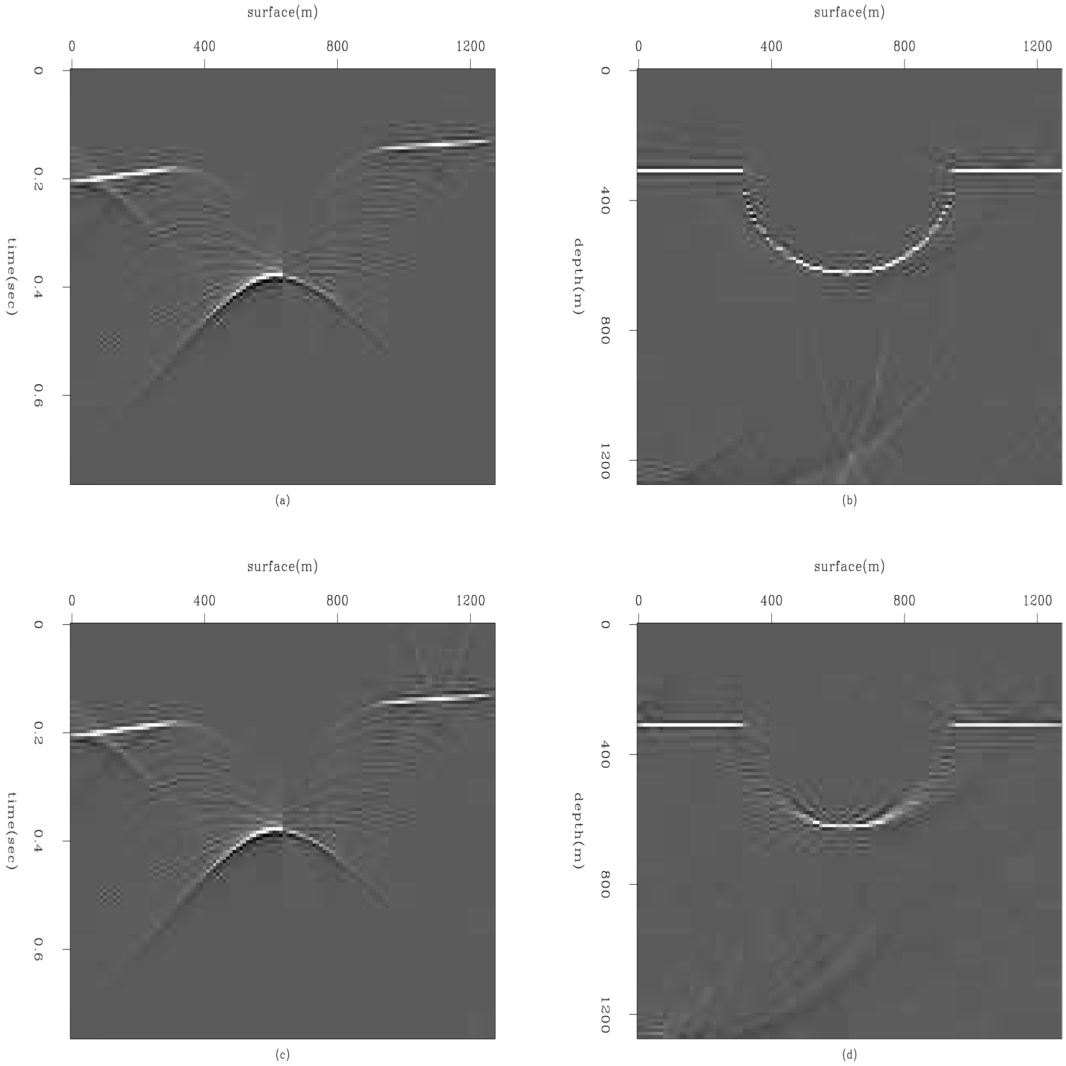

FIG. B.7. (a) Datumed wave field using split-step algorithm. (b) migrated image using split-step algorithm. (c) Datumed wave field using finite-difference algorithm. (d) migrated image using finite-difference algorithm. irrdtm-vxz-split-wxz-datum [R] datuming algorithm. The datuming algorithm using the finite-difference extrapolation is also tested for the same data, shown in Figure B.6(b); the datumed wave field is shown in Figure B.7(c) and the migrated image is shown in Figure B.7(d). In Figure B.7(d) we can see that the reflector is imaged correctly with the exception of the steep dip portion, which is limited by the 45-degree wave equation.

Bibliography

Al-Yahya, K. M., 1987, Velocity analysis by iterative profile migration: Ph.D. thesis, Stanford University.

Al-Yahya, K. M., 1989, Velocity analysis by iterative profile migration: Geophysics, **54**, no. 6, 718–729.

Berkhout, A. J., 1985, Seismic migration: Imaging of acoustic energy by wave field extrapolation: Elsevier, Amsterdam.

Berryhill, J. R., 1979, Wave-equation datuming: Geophysics, **44**, no. 8, 1329–1344.

Berryhill, J. R., 1984, Wave equation datuming before stack: 54th Annual Internat. Mtg., Soc. Expl. Geophys., Expanded Abstracts, Session:S2.6.

Berryhill, J. R., 1986, Submarine canyons: Velocity replacement by wave-equation datumin g before stack: Geophysics, **51**, no. 8, 1572–1579.

Biondi, B., 1990, Velocity analysis using beam stacks: Ph.D. thesis, Stanford University.

Bishop, T. N., Bube, K. P., Cutler, R. T., Langan, R. T., Love, P. L., Resnick, J. R., Shuey, R. T., Spindler, D. A., and Wyld, H. W., 1985, Tomographic determination of velocity and depth in laterally varying media: Geophysics, **50**, no. 6, 903–923.

Červený, V., 1987, Ray tracing algorithms in three-dimensional laterally varying layered structures *in* Nolet, G., Ed., Seismic Tomography:: Riedel Publishing Co., 99–134.

Claerbout, J. F., 1976, Migration in Media with Strong Lateral Velocity Variation: SEP–**8**, 1–7.

Claerbout, J. F., 1985, Imaging the Earth's Interior: Blackwell Scientific Publications.

Claerbout, J. F., 1994, Applications of three-dimensional filtering: SEP.

de Bruin, C. G., Wapenaarh, C. P. A., and Berkhout, A. J., 1990a, Imaging for angle-dependent reflectivity in the presence of dip: 60th Annual Internat. Mtg., Soc. Expl. Geophys., Expanded Abstracts, 1503–1506.

de Bruin, C. G. M., Wapenaar, C. P. A., and Berkhout, A. J., 1990b, Angle-dependent reflectivity by means of prestack migration: Geophysics, **55**, no. 9, 1223–1234.

Etgen, J., 1990, Residual prestack migration and interval velocity estimation: Ph.D. thesis, Stanford University.

Filho, C. A. C., 1992, Elastic modeling and migration in earth models: Ph.D. thesis, Stanford University.

Fowler, P., 1985, Zero offset prediction by polynomial interpolation: SEP–**42**, 83–96.

Fowler, P., 1988, Seismic velocity estimation using prestack time migration: Ph.D. thesis, Stanford University.

Gazdag, J., and Sguazzero, P., 1984, Migration of seismic data by phase shift plus interpolation: Geophysics, **49**, no. 2, 124–131.

Gazdag, J., 1978, Wave equation migration with the phase-shift method: Geophysics, **43**, no. 7, 1342–1351.

Inoue, H., 1986, A least-squares smooth fitting for irregularly spaced data: Fini te-element approach using the cubic B-spline basis: Geophysics, **51**, no. 11, 2051–2066.

Lumley, D., and Beydoun, W., 1991, Elastic parameter estimation by Kirchhoff prestack depth migr ation inversion: SEP–**70**, 165–192.

Lumley, D. E., Nichols, D., Ecker, C., Rekdal, T., and Berlioux, A., 1995, Amplitude-preserved processing and analysis of the Mobil AVO data se t: SEP–**84**, 125–152.

McMechan, G. A., 1983, Migration by extrapolation of time-dependent boundary values: Geophys. Prosp., **31**, no. 3, 413–420.

Neidell, N. S., and Taner, M. T., 1971, Semblance and other coherency measures for multichannel data: Geophysics, **36**, no. 3, 482–497.

Newman, P., 1973, Divergence effects in a layered earth: Geophysics, **38**, no. 3, 481–488.

Reshef, M., 1991, Depth migration from irregular surfaces with depth extrapolation methods: SHORT NOTE: Geophysics, **56**, no. 1, 119–122.

Rietveld, W. E. A., Berkhout, A. J., and Wapenaar, C. P. A., 1992, Optimum seismic illumination of hydrocarbon reservoirs: Geophysics, **57**, no. 10, 1334–1345.

Schultz, P. S., and Claerbout, J. F., 1978, Velocity estimation and downward-continuation by wavefront synthesis: Geophysics, **43**, no. 4, 691–714.

Shtivelman, V., and Canning, A., 1988, Datum correction by wave-equation extrapolation: Geophysics, **53**, no. 10, 1311–1322.

Stoffa, P. L., and Fokkema, J. T., 1990, Split-step Fourier migration: Geophysics, **55**, no. 4, 410–421.

Stork, C., 1988, Ray trace tomographic velocity analysis of surface seismic reflection data: Ph.D. thesis, California Institute of Technology.

Taner, M. T., and Koehler, F., 1969, Velocity spectra – digital computer derivation and applications of velocity functions: Geophysics, **34**, no. 6, 859–881.

Taner, M. T., 1976, Simplan: simulated plane-wave exploration: 46th Annual Internat. Mtg., Soc. Expl. Geophys., Expanded Abstracts, 186–187.

Tarantola, A., 1987, Inverse problem theory: Elsevier.

Toldi, J., 1985, Velocity analysis without picking: Ph.D. thesis, Stanford University.

van Trier, J., 1990, Tomographic determination of structural velocities from depth migrated seismic data: Ph.D. thesis, Stanford University.

Versteeg, R., and Grau, G., 1990, Practical aspects of seismic data inversion, the marmousi expe rience EAEG Workshop, 52nd EAEG Meeting, Eur. Assoc. Expl. Geophys., Proceedings of 1990 EAEG Workshop, 52nd EAEG Meeting, 1–194.

Whitmore, N. D., and Garing, J., 1993, Intervel velocity estimation using iterative prestack depth migration in the constant angle domain: The leading edge, **12**, no. 7, 757–762.

Wiggins, J. W., 1984, Kirchhoff integral extrapolation and migration of nonplanar data : Geophysics, **49**, no. 8, 1239–1248.

Yilmaz, O., and Lucas, D., 1986, Prestack layer replacement: Geophysics, **51**, no. 7, 1355–1369.

Zhang, L., 1990, Refining the image of profile migration: Residual moveout and residual migration: SEP–**65**, 17–28.